0273-2289/93/4101-2--0021$03.80

Microfabrication and Microsensors

SHUICHI SHOJI* AND MASAYOSHI ESASHI

Department of Mechatronics & Precision Engineering, Tohoku University, Sendai 980 Japan

ABSTRACT

In order to fabricate microsensors, a micromachining, microfabrication technique based on LSI technologies has been used. In this paper, useful micromachining techniques are described. Examples of integrated microsensors, such as a pressure sensor including a readout circuit and a multisensor cell for blood gas analysis, are introduced. Microflow control devices, such as a microvalve and a micropump for integrated chemical analysis systems, are also described.

Index Entries: Microsensors; micromachining; microfabrication; LSI technologies.

INTRODUCTION

Micromachining based on integrated circuits' microfabrication technologies, i.e. photolithography, etching, deposition, and so on, has been developed for the fabrication of three-dimensional (3D) microdevices. This technology allows the miniaturization of silicon based sensors (*1*). Integrated sensors consist of sensors and readout, and interface circuits are also fabricated by this technique. The encapsulation technique of the sensor is very important in practical use. Back gate ISFETs were developed considering easy encapsulation (*2,3*). For the packaging of microsensors, bonded silicon and Pyrex structures are very useful, having the advantages of small size and low cost. Integration of some sensors of the same chip, for example multiISFET flow cell, is another attractive application of micromachining (*2*). The multiISFET based biosensor is another example (*4*).

*Author to whom all correspondence and reprint requests should be addressed.

This report was presented at the US/Japan Workshop on Microfabrication and Biosensors, July 21–24, 1992, sponsored by the National Science Foundation.

Recently many microactuators have been developed, constituting a new field of application of micromachining (*5*). Microflow control devices, such as microvalves and micropumps, are the most useful applications of microactuators. Small size and negligible dead volume enables very fine flow control, on the order of 1 μL/min. An attractive application of these devices is the integration of conventional chemical analyzing systems on a silicon wafer (*6*).

This paper describes important techniques of micromachining, such as anisotropic wet etching and silicon-to-glass anodic bonding. Then examples of sophisticated microsensors, an integrated capacitive pressure sensor and a micro flow cell for blood gas analysis, are introduced. Finally, microflow control devices and a prototype of an integrated chemical analysis system are described.

MICROMACHINING

Silicon Etching

Silicon etching techniques are generally classified into two categories; isotropic etching and anisotropic etching. Each etching can be obtained by wet etching and dry etching. Nitric acid, fluoric acid, and acetic acid systems are generally used for isotropic wet etching. Since this etching shows large undercut and poor controllability of etching properties, it is difficult to apply when precise geometrical control is necessary. Dry etching techniques, such as plasma etching and reactive ion etching, have not been used very often for deep balk etching because of their small etch rate.

Anisotropic Wet Etching

Anisotropic wet etching plays a very important role in micromachining. Fine 3D microstructures, i.e., cantilever bridge, diaphragm and so forth, have been fabricated as shown in Fig. 1. Some kind of alkaline hydroxide or organic aqueous solutions have been used as the etchants. Potassium hydroxide, ethylendiamine, and hydrazine are typical. The important properties of this etching technique are anisotropic, selectivity, handling, nontoxicity, and process compatibility. Ammoniumhydroxide-water (AHW) and quaternary ammoniumhydroxide-water (QAHW) solutions have recently been developed to obtain integration circuit compatibility. The characteristics of these etchants are summarized in Table 1.

Alkaline Metal Hydroxide

Purely inorganic alkaline solutions, like KOH, NaOH, and LiOH, have been used for the etchant (*7,8*). The effect of different anions are minor if solutions of same molarity are used. KOH solutions are most commonly used and their etching procedures were studied in detail.

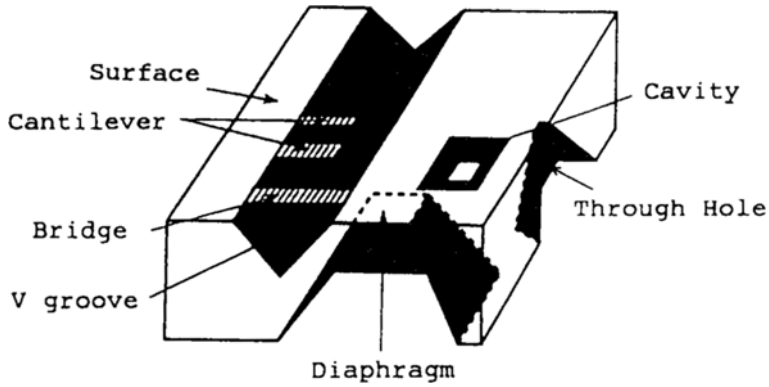

Fig. 1. Microstructures fabricated by wet aniostropic etching.

Table 1
Characteristics of Silicon Anisotropic Etching

Etchant	Etch rate (μm/min)	(100)/(111) Ratio	(110)/(111) Ratio	Etch rate SiO_2 (Å/min)
KOH Water (35 wt%)	1.0 (80°C)	400	600	14
CsOH Water (60 wt%)	0.15 (50°C)	-	200	0.25
EPW* +Pyrazine	1.25 (115°C)	35	-	2
Hydrazine Water (1:1)	3.0 (100°C)	16	9	1.7
AHW** (4 wt%)	0.7 (50°C)	-	200	8
TMAHW*** (22 wt%)	1.0 (90°C)	33	-	24

*EPW: Ethylenediamine-Pyrocatechol-Water
**AHW: Ammoniumhydrooxide-Water
***TMAHW: Tetramethyl ammonium hydroxide-Water

Uniform and constant etching can be realized with highly concentrated KOH of above 20 wt% at above 60°C. These etchants are less toxic, but the etch rate of silicon dioxide is large compared to the other etchants.

Organic Aqueous Solutions

Ethylendiamine pyrocatechol water (EDP) and Hydrazine water are the typical etchants for this category (*7,9*). The primitive etchant of the EDP system consists of ethylenediamine and water. The addition of pyrocatechol causes a large increase in the etching rate. Purging the etching

chamber with an inert gas is necessary during etching. Adding pyrazine to the solution makes the etch rate constant. This etchant has very high selectivity between silicon and SiO_2, which is one of the remarkable advantages. The etch rate ratios of (100)/(111) and (110)/(111) are small compared to those for the pure alkaline solutions.

Hydrazine and water, normally 1:1 solution, has similar etching properties to the EDP solution; for example, it also has a small etch rate and a small orientation dependency. The etching rate is about two times larger than that of EPW. The pyramidal shaped etch pits are sometimes observed in this etching. Ag, Au, Ti, and Ta withstand this etching solution, whereas Al, Cu, and Zn are attacked. EDP and hydrazine are carcinogens (*9*).

Ammoniumhydroxide-water (AHW) solution and quarternaly ammoniumhydroxide-water (QAHW) solutions have been developed considering integrated compatability (*10,11*).

AHW shows similar orientation selectivity to EDP etchants. The (100) etching front is covered with etch pits. These etch pits can be suppressed by adding small amounts of H_2O_2 (*10*). Aluminum is not attacked by silicon-doped AHW.

Tetramethylammoniumhydroide-water (TEAHW) and Tetramethylammoniumhydroide-water (TMAHW) have similar etching characteristics (*11*). The maximum (100) etch rate appeared at 20 wt% for TEAH and appeared at 5 wt% for TMAH. The etch pits had low QAH concentration. It appeared below 20 wt% in TEAHW and appeared below 15 wt% in TMAHW. The selectivity of SiO_2 to (100) to (111) of QAH is high and increases with decreasing temperature.

Etching Stop (Selective Etching)

Some kinds of doping-selective, bias-controlled etching techniques have been developed. In anisotropic etching, these selective etching techniques are simply classified into two categories as shown in Fig. 2. One uses highly boron-doped silicon and the other uses the biased *p–n* junction.

P^+ Etch Stop

All alkaline anisotropic etchants exhibit a strong reduction of their etch rate at high boron concentrations (*8*). The group of purely alkaline hydroxide solutions, like KOH and NaOH, and the group of aqueous solutions of organic substances, like EDP and Hydrazine, show different properties. The former group shows high alkaline concentration dependency of etch rate reduction on boron concentration. The latter group generally shows smaller etch rate for a boron-doped layer than the former group.

P–N Junction Etch Stop

There are some methods of *p–n* junction etch stop using 2, 3, or 4 electrodes (*12,13*). Equipment using a typical 4-electrodes method with a reference electrode, a counter electrode, and *n*- and *p*-type silicons themselves, is shown in Fig. 3 (*13*). The etch-stop is caused by the well known

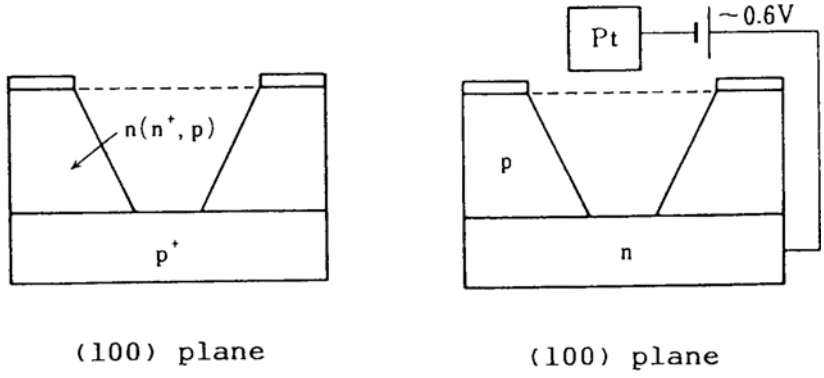

Fig. 2. Etching stop methods in anisotropic etching.

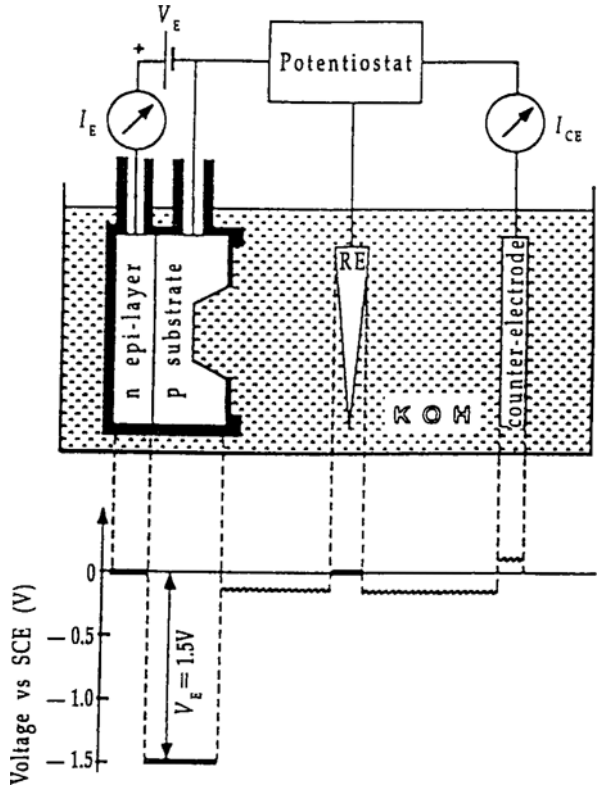

Fig. 3. Schematic setup for *p–n* junction etch stop (*13*).

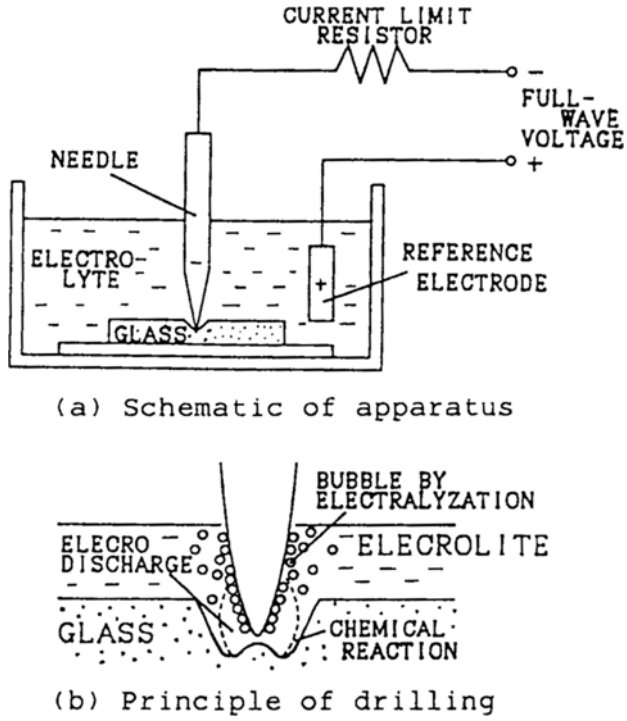

Fig. 4. Schematic setup and principle of the electro-chemical discharge drilling.

anodic oxidation, which stops the etching. The reverse-bias *p–n* junction can provide a large selection of the *p*-type silicon over the *n*-type in anisotropic etching solutions. The negative voltage is applied to prevent oxidation on the *p*-type silicon surface, whereas the positive voltage is applied to the *n*-type silicon to be anodically oxidized when the *p*-type silicon is etched completely. In the 3-electrode system, the *p*-type silicon floats electrically while it is being etched. The etch stop is obtained in both alkaline hydroxide solutions and organic aqueous solutions.

Etching and Drilling of Pyrex

In order to fabricate sophisticated sensors, micromachining of Pyrex has also been necessary. Pyrex can be etched by concentrated HF using Cr–Au as a mask (*14*). The etching profile is isotrophic. Electrodischarge drilling, a traditional ceremic machining technique, is useful for boring very fine through-holes (*14*). The schematic setup and principle of drilling are shown in Fig. 4. The glass is placed in alkaline hyroxide solution. A fine needle is put on the glass and negative voltage (around 40 V) is applied. The discharge occurs at the tip, which increases the temperature locally. The glass at the tip is removed by thermally accelerated chemical etching. An example of the needle and the hole is illustrated in Fig. 5. Smooth etching surface is achieved when highly concentrated NaOH solution of larger than 35 wt% is used.

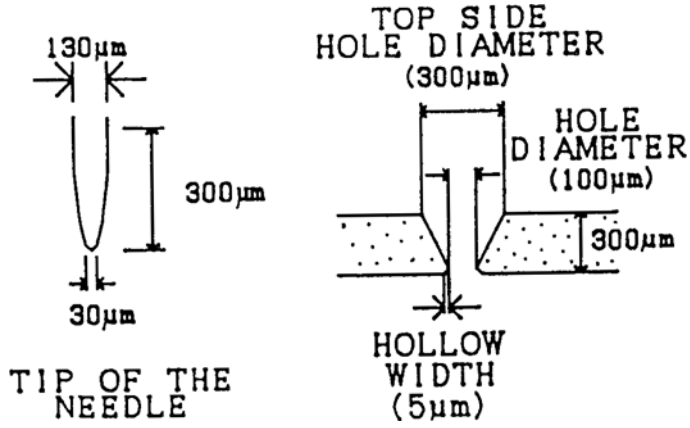

Fig. 5. Cross-sectional view of a needle and a hole.

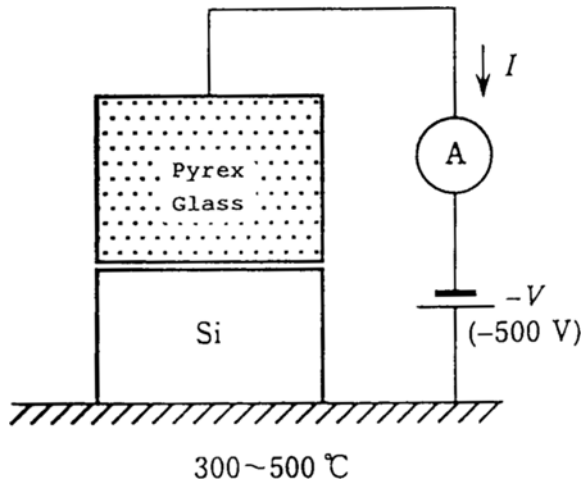

Fig. 6. Schematic setup of the anodic bonding.

Anodic Bonding

Anodic bonding of silicon to Pyrex is the most popular method of bonding, and is useful for fabricating hermetically-sealed microstructures. The schematic setup of the bonding is shown in Fig. 6. The bonding has been done under 400°C applying negative voltage of 500–1000 V to the glass. Since the thermal expansion coefficients of silicon and Pyrex are close to each other over the bonding temperature range, the residual stress after bonding is small. This is the reason why Pyrex has been used for this purpose.

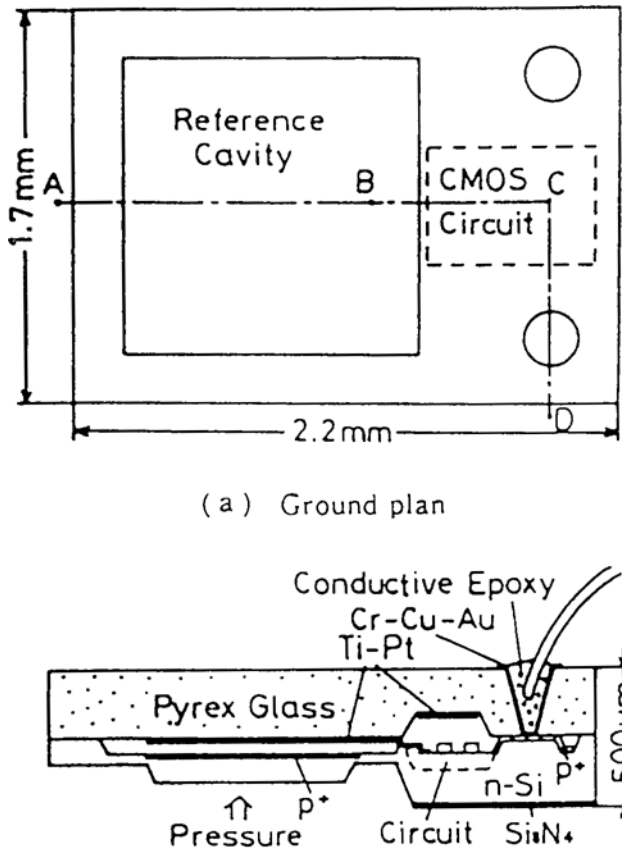

(a) Ground plan

(b) Cross section of *A-B-C-D*

Fig. 7. Integrated capacitive type pressure sensor.

INTEGRATED SENSORS

Integrated Capacitive Pressure Sensor

Integration of sensors and circuits for readout and interface is the primary approach of more sophisticated sensors. Fig. 7 shows the structure of an integrated absolute capacitive pressure sensor (*15*). It consists of anodically-bonded silicon and glass substrates with hermetically sealed reference cavities. The pressure is detected by the capacitance change between the silicon diaphragm and aluminum electrode formed on the glass. A capacitance-to-frequency converter readout of the CMOS circuit is integrated on the silcon substrate. In this case, the chip itself is a package unit because the sensor and circuit are shielded from the surrounding environment. This structure enables the packaging to be completed at wafer level by batch fabrication. Similar hermetically sealed structures are useful for accelerometers, resonant sensors, and so on (*16,17*).

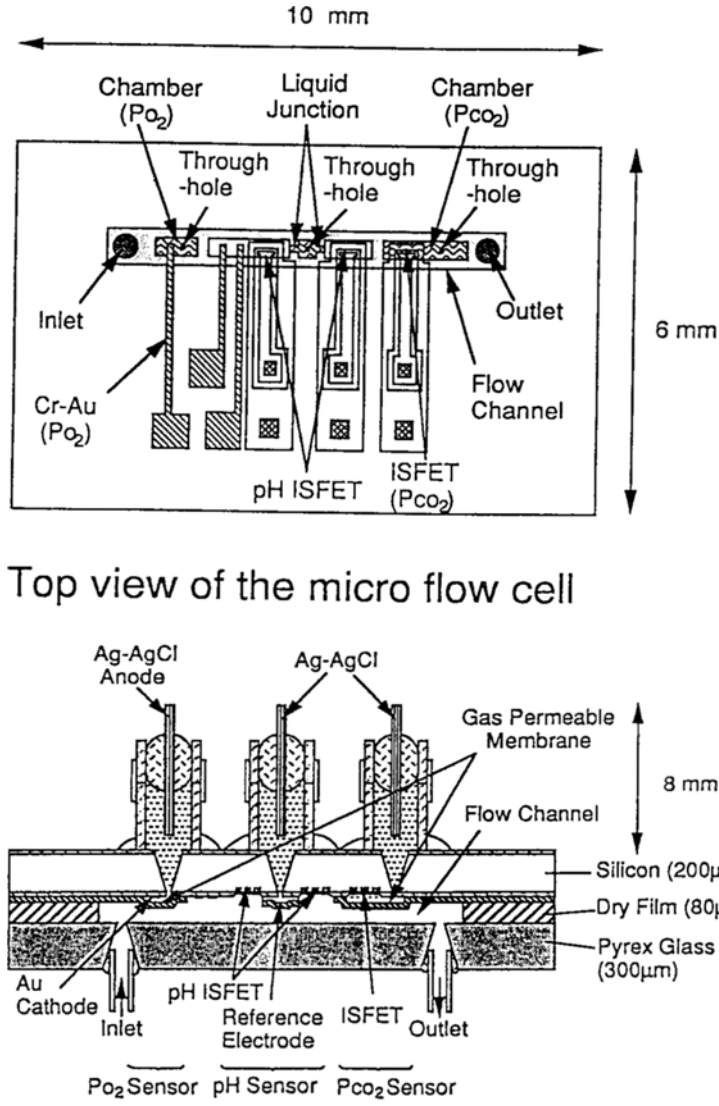

Fig. 8. Structure of the flow cell for blood gas analysis.

Microflow Cell for Blood Gas Analysis

To create a blood gas analysis system, a microflow cell that has a PO_2 sensor, a PCO_2 sensor, and two pH ISFETs has been developed (*18*). The structure of the microflow cell is illustrated in Fig. 8. The PO_2 sensor is a small Clark-type electrode, which consists of a thin Cr–Au cathode and an Ag–AgCl wire (0.3 mmϕ) anode. The PCO_2 sensor is a miniaturized

Severing-house-type sensor using ISFET as a pH electrode. A negative photoresist thin film about 1 μm thick (Tokyo Ohka OMR-83) was used as the gas permeable membrane. A very small chamber of 1 μm in thickness is formed between the membrane and the silicon substrate. The pH sensor is a Si_3N_4 gate ISFET. The reference electrode consists of a liquid junction and an Ag–AgCl wire electrode. Three Ag–AgCl reference electrodes are placed on the back side of the silicon wafer. The sample inlet and outlet are formed on the glass. The silicon wafer and the glass are bonded with a photosensitive dry film (Hitachi Kasei Co., catalog no. SR-1300G). A flow channel of 600 μm in width, 7 mm in length, and 80 μm in thickness is formed in the dry film. The necessary sample volume was reduced to about 0.34 μL with this structure.

MICROFLOW CONTROL DEVICES

Microvalve

The structure of a three-way microvalve using a stack piezoelectric actuator is shown in Fig. 9 (*19*). A glass plate is sandwiched between two silicon wafers. The upper wafer has a diaphragm that has two mesa structures: a center mesa and a surrounding mesa. A piezoelectric actuator is placed on the center mesa and its holder is glued to the surrounding mesa with a glass pipe. A freestanding Ni gasket is formed on the surrounding mesa. Liquid from inlet 2 flows through a gap between the inside valve seat and the glass while liquid from inlet 1 is stopped at the surrounding valve seat. When voltage is applied, the actuator pushes down the inside valve seat to the glass and the surrounding valve seat is lifted. Then liquid is introduced from inlet 1 through the gap and the flow from inlet 2 is shut off.

Micropump

The structure and operating principle of a typical micropump driven by a piezoelectric stack are illustrated in Fig. 10 (*20*). It is constructed with two glass plates and a silicon wafer. A pressure chamber and a mesa suspended with a thin diaphragm are formed on the upper glass plate. A piezoelectric actuator is placed on the mesa. Two check valves made of poly-silicon are fabricated on the silicon wafer at the inlet and the outlet of the pressure chamber. When voltage is applied to the actuator, liquid flows to the outlet (pumping mode). As the voltage is cut off, liquid flows into the pressure chamber from the inlet (suction mode). Pumping is carried out by driving the actuator with periodic voltage.

Two kinds of constant and rippleless pumps have been developed (*20*). One is a dual pump consisting of two micropumps connected in parallel, which are driven with complementary periodic two-phase voltage. The other is a buffer pump that has a synchronous buffer connected

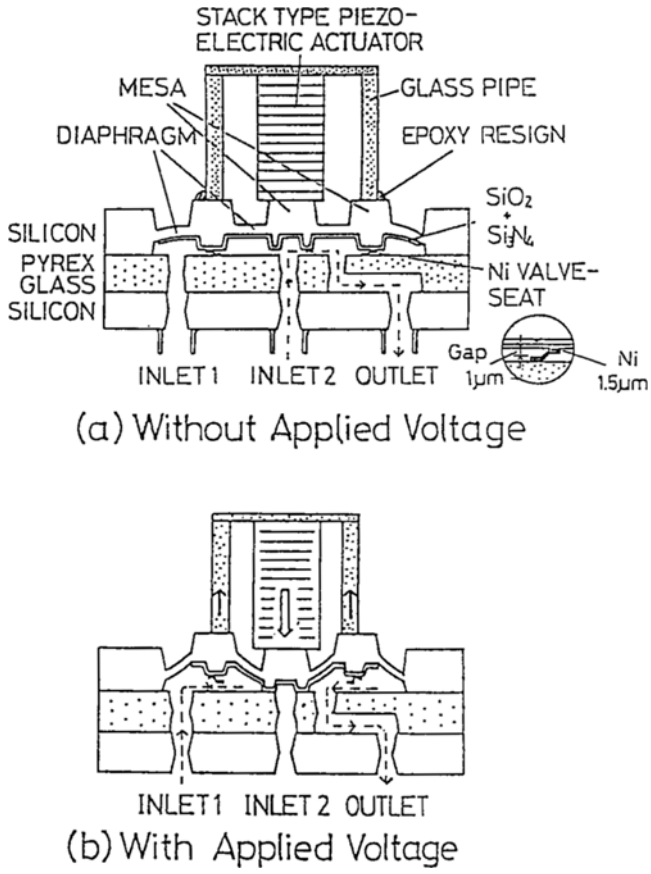

Fig. 9. Structure of the stack type three-way microvalve.

in series with a pump. The synchronous buffer is driven with the pump. Fig. 11 shows the load characteristics of the micropump. This micropump has an output pressure of about 0.15 atm.

Prototype of Integrated Chemical Analyzing System

The first prototype of an integrated FIA was demonstrated using a stacked silicon and glass structure (*19*). Its principle and structure are illustrated in Fig. 12. It is about 20 mm × 20 mm × 10 mm in size. The system has two micropumps, a sample injector and a reaction coil, making it one of the simplest FIA systems. The sample injector consists of two three-way microvalves and a sample channel. Each element in this system needs to be improved and the detector flow cell must be integrated. Nevertheless, this prototype demonstrates that some sophisticated chemical analyzing systems can be fabricated on a silicon wafer.

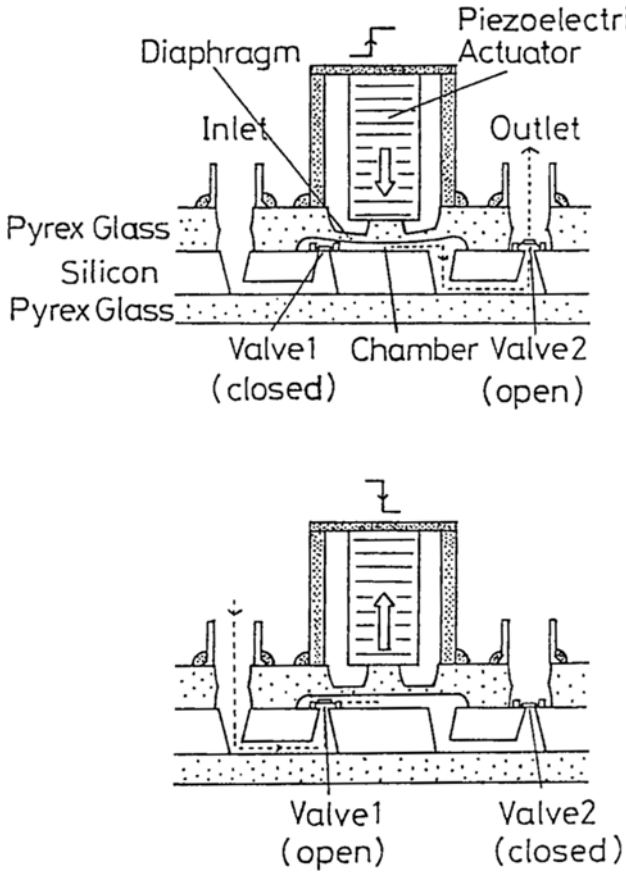

Fig. 10. Structure and principle of the micropump using poly-silicon check valves.

CONCLUSION

Basic techniques of micromachining, etching, and bonding were described. Micromachining is also applicable for not only miniaturization but also low cost encapsulation by batch process packaging. The micro-packaging structure can be also applicable for biosensors. Microflow cell including different types of gas sensors are also fabricated by micro-machining. This represents a wide possibility of integrated multisensors. This kind of integration technique also can be applied for multibiosensor systems.

New approaches for realizing integrated chemical analyzing systems are being introduced. In the near future, these integrated systems will be perfected and contribute to advanced biosensing systems.

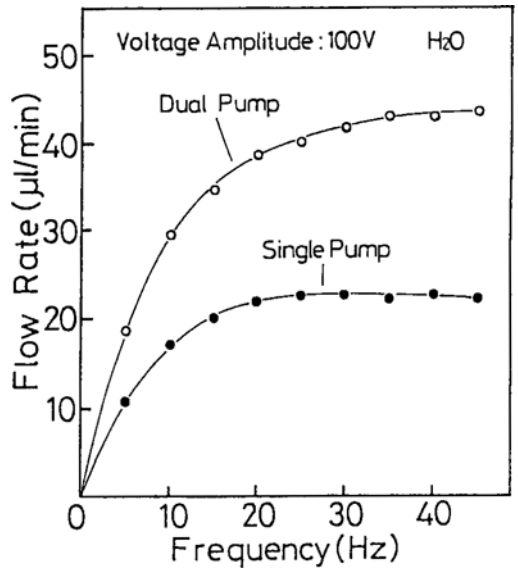

Fig. 11. Load characteristics of the micropump.

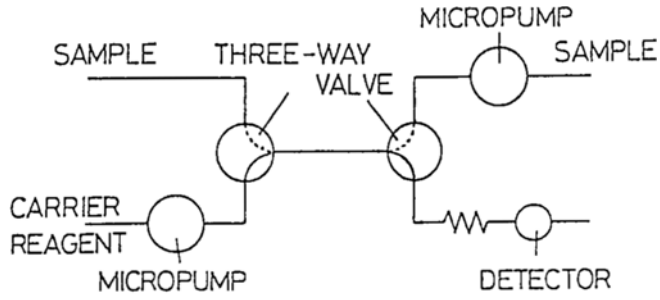

(a) PRINCIPLES OF FIA

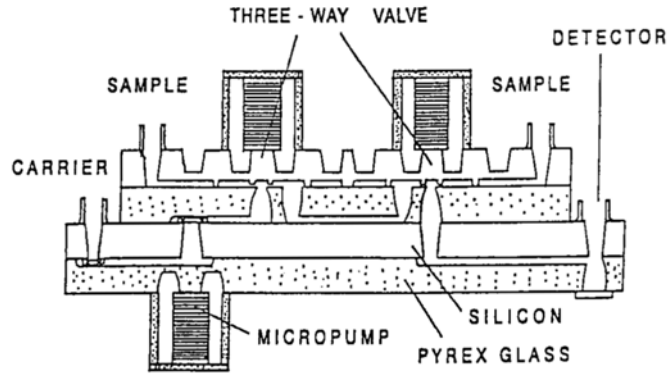

(b) A STRUCTURE OF AN INTEGRATED FIA SYSTEM

Fig. 12. Principle and structure of the prototype of the integrated FIA system.

REFERENCES

1. Fung, C. D., Cheung, P. W., Ko, W. H., and Fleming, D. G. (1985), *Micromachining and Micropackaging of Transducers*, Elsevier, Amsterdam.
2. de Rooij, N. F. and Van den Vlekkert, H. H. (1991), *Chemical Sensor Technology* **3,** 213.
3. Sakai, T., Amemiya, I., Uno, S., and Katsura, M. (1990), *Sensors and Actuators* **B1,** 341.
4. Kimura, J., Kuriyama, T., and Kawana, Y. (1986), *Sensors and Actuators* **9,** 373.
5. Peterson, K. E. (1992), *Proc. IEEE*, vol. 70, 420.
6. Shoji, S., Esashi, M., and Matsuo, T. (1988), *Sensors and Actuators* **14,** 101.
7. Seidel, H., Csepregi, L., and Heuberger, A. (1990), *J. Electrochem. Soc.* **137,** 3612.
8. Siedel, H., Csepregi, L., and Heuberger, A. (1990), *J. Electrochem. Soc.* **137,** 3626.
9. Mehregany, M. and Senturia, S. D. (1988), *Sensors and Actuators* **13,** 375.
10. Schnakenbeg, U., Benecke, W., and Lochel, B. (1990), *Sensors and Actuators* **A21–A23,** 1031.
11. Tabata, O., Asahi, R., Funabashi, H., and Sugiyama, S. (1991), *Tech. Dig. Int. Conference on Solid-State Sensors and Actuators Transducers '91* pp. 811.
12. Linden, Y., Tenerz, L., Tiren, J., and Hok, B. (1989), *Sensors and Actuators* **16,** 67.
13. Kloeck, B., Collins, S. D., de Rooij, N. F., and Smith, R. L. (1989), *IEEE Trans. Elect. Dev.* **ED-36,** 663.
14. Shoji, S. and Esashi, M. (1990), *Tech. Dig. 9th Sensor Symposium*, pp. 27.
15. Esashi, M., Ura, N., and Matsumoto, Y. (1992), *Proc. Micro Electro Mechanical Systems MEMS'92*, Travemunde, pp. 43.
16. Kudoh, T., Shoji, S., and Esashi, M. *Sensors and Actuators A,* **29,** 185.
17. Yoshimi, K., Minami, K., Wakabayashi, Y., and Esashi, M. (1992), *Tech. Dig. 11th Sensor Symposium*, Tokyo, pp. 35.
18. Shoji, S. and Esashi, M. (1992), *Sensors and Actuators B,* **8,** 205.
19. Nakagawa, S., Shoji, S., and Esashi, M., (1990), *Proc. of IEEE Workshop of Micro Electro Mechanical Systems*, Napa Valley, CA, pp. 89.
20. Shoji, S., Nakagawa, S., and Esashi, M. (1990), *Sensors and Actuators* **A21–A23,** 189.